

THE INFLUENCE OF FRICTION FORCE AND HYSTERESIS ON THE DYNAMIC RESPONSES OF PASSIVE QUARTER-CAR SUSPENSION WITH LINEAR AND NON-LINEAR DAMPER STATIC CHARACTERISTICS

Zbyszko KLOCKIEWICZ*, Grzegorz ŚLASKI*

*Faculty of Mechanical Engineering, Institute of Machine Design, Poznan University of Technology, ul. Piotrowo 3, 61-138, Poznan, Poland

zbyszko.klockiewicz@put.poznan.pl, grzegorz.slaski@put.poznan.pl

received 8 August 2022, revised 11 January 2023, accepted 22 January 2023

Abstract: Vehicle passive suspensions consist of two major elements generating force – spring and passive damper. Both possess non-linear characteristics, which are quite often taken into account in simulations; however, the friction forces inside the hydraulic damper and the damping force's hysteresis are usually left out. The researchers in this paper present the results of examination of the influence of using complex damper models – with friction and hysteresis; and with linear and non-linear static characteristics – on the chosen dynamic responses of a suspension system for excitations in the typical exploitation frequency range. The results from the simulation tests of the simplified and advanced versions of the damper model – different transfer functions and their relation to the reference model's transfer functions – are compared. The main conclusion is that friction and hysteresis add extra force to the already existing damping force, acting similar to damping increase for the base static characteristics. But this increase is not linear – it is bigger for smaller frequencies than for higher frequencies. The research shows the importance of including non-linear characteristics and proposed modules in modelling passive dampers.

Key words: vehicle vertical dynamics, damper model, friction, hysteresis, transfer function

1. INTRODUCTION

The car suspension – in a sense of mechanical components – is a group of elements such as springs, shock absorbers and linkages that connect the vehicle body or frame to its wheels and transmit longitudinal, lateral and vertical forces between them while simultaneously allowing relative vertical motion between the wheel and the body or frame of the vehicle.

In the sense of functionality in an area of vehicle vertical dynamics, the suspension must support both road holding/handling and ride quality, which are at odds with each other. The structure of suspension, wheels and the body forms an oscillatory system, affected by kinematic excitation z_r caused by the road surface profile (Fig. 1) and also by the force excitations caused by inertial forces acting on vehicle body during manoeuvres in the longitudinal or lateral directions (1).

In detail, the functionality of the suspension in the area of vertical dynamics involves keeping the car wheel in contact with the road surface as much as possible, because all the road or ground forces acting on the vehicle do so through the contact patches of the tyres. The suspension also protects the vehicle itself and any cargo or luggage from damage and wear, working as a vibration isolation system that minimises the effects of road kinematic excitations.

The kinematic excitations processed by the suspension's dynamic structure produce responses such as bounce displacement of the sprung mass z_M and the unsprung mass z_m ; the relative displacement of both masses – the suspension deflection (rattle

space) $z_M - z_m$; the acceleration of the sprung and unsprung masses (\ddot{z}_M, \ddot{z}_m); as well as the forces F_t of tyre-road contact. The relations between road excitation and listed suspension responses, in a function of excitation frequency, usually are called suspension transmissibility functions (2), the dynamic characteristics of suspension, the frequency response function or the magnitude-frequency characteristics (3,4).

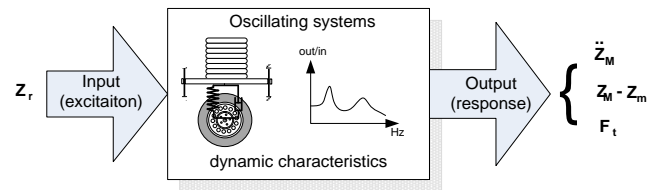


Fig. 1. A car suspension as an oscillatory system with its dynamic characteristics

The shape and amplitude values of the frequency response functions (transfer functions) allow the easy assessment of suspension performance in terms of the criteria of comfort, safety and suspension rattle space, which is a technical limitation of suspensions. Ride comfort can be assessed using the sprung mass acceleration transfer function $\ddot{z}_M(\omega)$, the safety potential using the dynamic wheel load transfer function $F_t(\omega)$ and technical limitations with the wheel rattle space amplification function. This function is also important from the point of view of the kinematic performance of the suspension – possible changes of wheel camber

and steer angles – and the influence of vertical dynamics on lateral dynamics.

These functions can be shaped by tuning the parameters of the suspension components – sprung and unsprung masses, spring characteristics and shock absorber (damper) characteristics and the tyre stiffness and damping coefficients or characteristics. Thus, it can be said that synthesis of suspension performance involves finding the right compromise between fulfilling all the tasks in terms of vertical dynamics by setting adequate suspension stiffness and damping parameters or characteristics to fulfil all the tasks in an optimised way.

A lot of research concerning improving the ride comfort and handling performance has been done purely on theoretical, simplified models of vehicle vertical dynamics, usually linear, where the stiffness and damping characteristics are described by only linear parameters. This method of modelling suspensions is justified when using shock absorbers and springs with linear characteristics in earlier periods of motor car history and also while narrowing the range of analysis only to the use of the linear part of the spring or characteristics of the shock absorber. Finally, the use of linear parameters could be justified by the use of substitute linear parameters in place of real non-linear characteristics.

The experimental tests of shock absorber characteristics show that not only are non-linear static characteristics often not implemented in simple mathematical models but also additional phenomena, such as dry friction or hysteresis in a suspension, are not considered.

Thus, more advanced models include non-linear characteristics and/or asymmetrical characteristics. Sometimes, dry friction is added (5–7), while taking into account damping force hysteresis is rare. The authors therefore decided to research the influence of inclusion of friction and hysteresis modules into the shock absorber model on changes in the estimated frequency responses of suspensions with linear and non-linear static shock absorber characteristics.

2. RESEARCH METHOD

2.1. Research matrix and model parameters

In the research, computer simulation of a vertical dynamics model of a quarter car was implemented in MatLab/Simulink software. Specifically, modified quarter-car models with different damper models were used for the different cases, as presented in Tab. 1.

Tab. 1. Shared features of a quarter-car model used in the research

Case no.	Linear characteristic	Non-linear characteristic	Friction	Hysteresis
1	✓	–	–	–
2	✓	–	✓	–
3	✓	–	–	✓
4	✓	–	✓	✓
5	–	✓	–	–
6	–	✓	✓	–
7	–	✓	–	✓
8	–	✓	✓	✓

The investigation began by analysing Case 1 – the simplest possible damping characteristic – passive linear one with minimum (900 Ns/m) and maximum (3,100 Ns/m) damping coefficient. The case involving just the non-linear static characteristic without friction and hysteresis, namely Case 5, was chosen as the easiest way to model real damper characteristics in both maximum and minimum damping modes (Fig. 4). Cases 2–4 and 6–8 were also tested as passive suspension, with constant shock absorber static damping characteristics but including additionally either friction or hysteresis, or both of them.

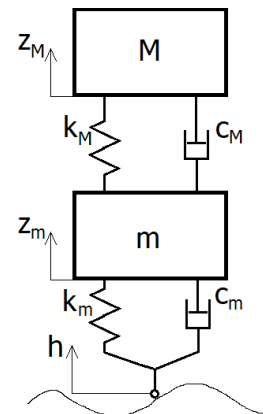


Fig. 2. Quarter-car model used in the simulations

The notations in the figure mean: M – the sprung mass, m – the unsprung mass, k_M – the suspension stiffness coefficient, k_m – the tyre stiffness coefficient, c_M – the suspension damping coefficient, c_m – the tyre damping coefficient, z_M – the sprung mass displacement, z_m – the unsprung mass displacement, h – the kinematic excitation.

All other suspension parameters were shared between all versions of the model: the linear stiffness characteristics of a tyre and suspension were used (Tab. 2), while the quarter-car model used is shown in Fig. 2.

Tested models were subjected to the excitation that enables calculation of the suspension dynamic responses in the form of transfer functions (frequency response function) between excitation and responses important for evaluation of suspension dynamic performance:

- suspension deflection for evaluation of necessary rattle space;
- sprung mass acceleration and sprung mass displacement for evaluation of ride comfort;
- cumulative tyre force for evaluation of safety potential.

Tab. 2. Shared features of a quarter-car model used in the research

Parameter	Unsprung mass	Sprung mass	Tyre stiffness	Tyre damping	Suspension stiffness
Unit	(kg)	(kg)	(kN/m)	(Ns/m)	(kN/m)
Value	50	400	200	350	30

The road excitation used in the research was a vertical sinusoidal displacement with a constant amplitude of 3 mm and a variable frequency starting from 0.0001 Hz up to 40 Hz (Fig. 3). It is similar to that used in European Shock Absorber Manufacturers Association (EUSAMA) testers during periodical technical inspections of car suspensions.

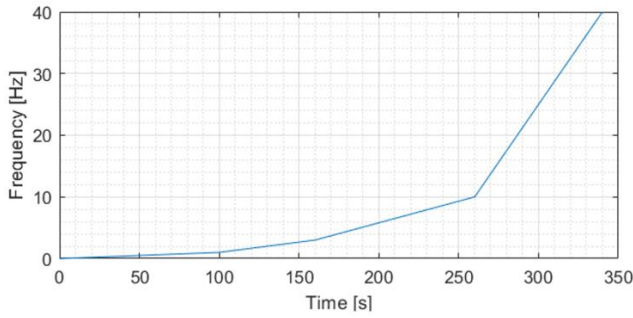


Fig. 3. Changes in the frequency of the input signal over simulation time

Important frequencies when analysing suspension dynamics cover a range from 0.5 Hz to 25 Hz. The frequency values changed in a non-linear fashion in order to allow more cycles to occur in a lower range, which gives better results when calculating transfer functions (8). Additionally, frequencies <0.5 and >25 Hz were added to the simulation in order to further stabilise the results of the tfestimate MatLab function, which was used to estimate the transfer function of the suspension.

2.2. Damper models including friction and hysteresis

The damper model for all cases, besides Case no. 1 (labelled as "linear"), had non-linear, asymmetric characteristics identified after empirical testing of damping forces of a real damper and averaging these forces to obtain the static characteristics (9) (Fig. 4).

All the damper model versions, besides Case no. 1, included a model of an adjustable damper with hysteresis, friction and also actuation delay modelled but not used in this research (Fig. 5).

Four main modules were applied to model the total damper force:

1. the static damping force,
2. hysteresis force,
3. friction force and
4. dynamic response.

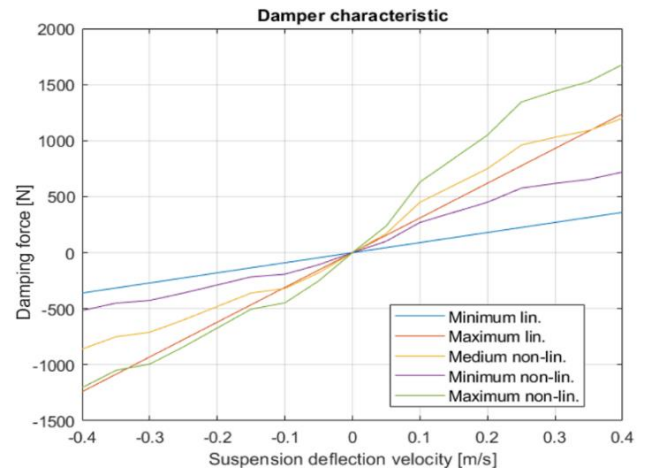


Fig. 4. Damper model static characteristics; lin. – linear, non-lin. – non-linear

The static damping characteristics module models the damping force as a function of deflection speed, differing for the compression and rebound and also on the control current if it models the electrically adjusted damper. Its implementation in Simulink is shown in Fig. 6.

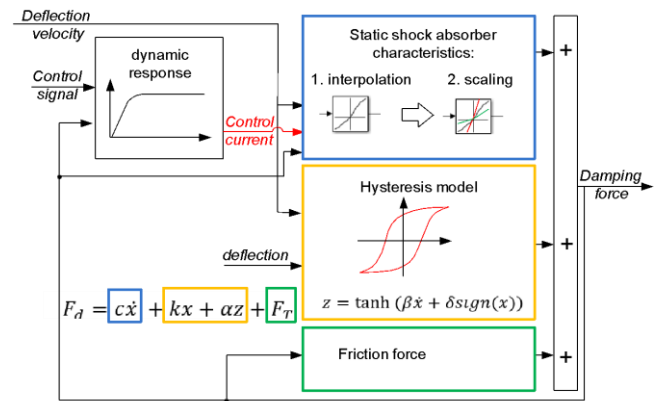


Fig. 5. Damper model diagram

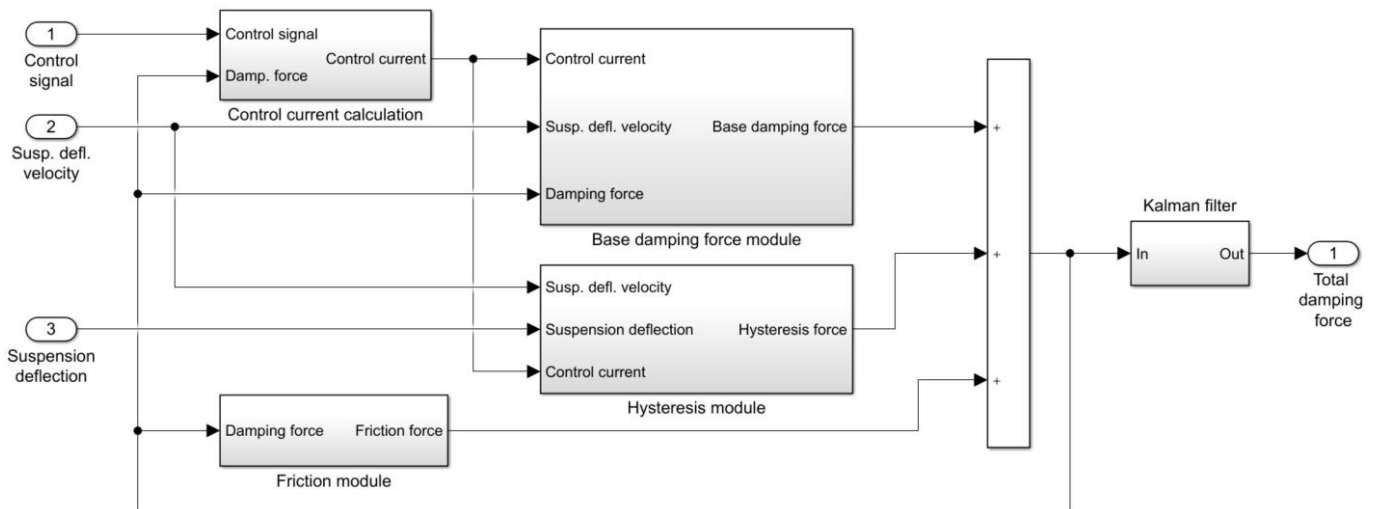


Fig. 6. Advanced damper simulation model
Damp. – Damping; Susp. defl. – Suspension deflection

For linear and symmetrical characteristics, the damping force can be modelled using simple equations (it was done for linear damper for Case no. 1):

$$F_d = c\dot{x}, \tag{1}$$

where c is the damping coefficient and \dot{x} is the damper compression/extension velocity.

In cases of non-linear and asymmetrical characteristics (cases no. 2–4 and 6–8), interpolation of experimental characteristics was used by using the “Look-up table” block during MatLab/Simulink software implementation.

For the adjustable damper, the interpolation was also necessary for the value of damping force in relation to the control current. This also can be accomplished with two-dimensional “Look up table” block for the three-dimensional shock absorber characteristics. Assuming a linear relation between the control current and the damping forces, the medium damping F_{dS_m} static characteristic was used along with the coefficient K_I to increase or decrease damping force according to the value of the valve coil

current and the state of the damper work – compression or rebound:

$$F_{dS_I} = F_{dS_m} \cdot K_I, \tag{2}$$

where: F_{dS_I} – interpolated value of damping force from the static characteristic for a given current, F_{dS_m} – the middle static characteristics damping force (for middle value of valve coil current), K_I – the coefficient to increase or decrease the damping force according to the value of valve coil current and state of damper work – compression or rebound. K_I values for the modelled shock absorber formulas, according to the value of the current I_c ($0.6 \leq I_c \leq 1.6$ A), were determined respectively for compression and rebound as follows:

$$K_{IC} = -0.55I_c + 1.59 \tag{3}$$

and

$$K_{IR} = -0.71I_c + 1.74 \tag{4}$$

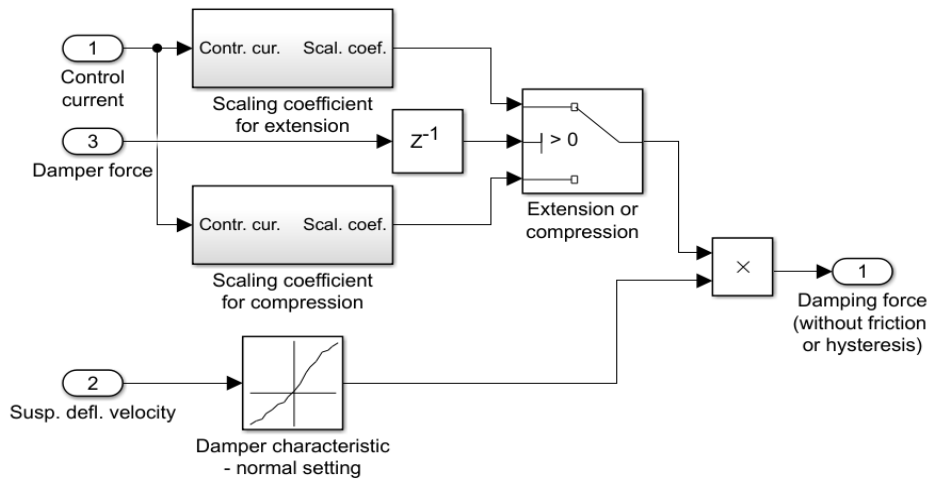


Fig. 7. Base damping force calculation subsystem

Contr. cur., control current; Scal. coef., scaling coefficient; Susp. defl., suspension deflection

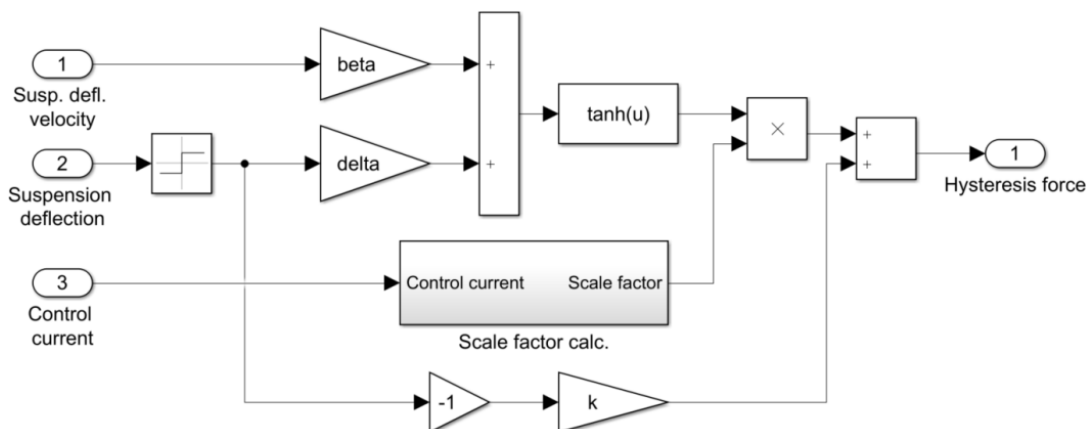


Fig. 8. Hysteresis module of the Simulink damper model

calc., calculation; Susp. defl., suspension deflection

The damper hysteresis module (Fig. 8) is important for high damping forces and high velocities. A simple model based on a previous work (10) was proposed to simulate the hysteretic force–velocity characteristic of the damper. This model is given by the

following formulas:

$$F_h = kx + \alpha z, \tag{5}$$

$$z = F_0 \cdot \tanh(\beta\dot{x} + \delta \text{sign}(x)), \tag{6}$$

where: k – the stiffness coefficient, which is responsible for the hysteresis opening found from the vicinity of zero velocity; a large value of k corresponds to the hysteresis opening of the ends; z – the hysteretic variable given by the hyperbolic tangent function; β – the scale factor of the damper velocity defining the hysteretic slope; a large value of β gives a steep hysteretic slope. δ – factor determining the width of the hysteresis through the term $\delta \text{sign}(x)$; a wide hysteresis results from a large value of δ , α – scale factor of the hysteresis that determines the height of the hysteresis; its value depends on the control current.

Based on the dynamic characteristic analysis of the tested shock absorber, a formula for the relation between scale factor α and valve coil current I_C was developed as follows:

$$\alpha = \alpha_0 \cdot (-2.15I_C + 4.45) \quad (7)$$

where: α_0 – scale factor α of the hysteresis for middle static characteristics damping force.

The hysteresis force's value was dependent on the suspension deflection and its velocity, as well as on the control current's value and a number of empirically obtained parameters [9].

The internal friction module (Fig. 9) models the force F_T and consists of two elements – the value of the kinetic friction force and a signum function due to the model friction force with opposite sign to the damping force. The friction force calculation depends on the suspension deflection velocity: if it was greater than a given threshold, then the friction force had a value equal to the defined kinematic friction (35 N); if it was smaller, then the kinematic friction value was multiplied by the ratio of current suspension deflection velocity to the threshold value.

$$F_f = \begin{cases} 35 \text{ if } v_{defl} > 0.1 \text{ m/s} \\ 35 \cdot \frac{v_{defl}}{0.1} \text{ if } v_{defl} < 0.1 \text{ m/s} \end{cases} \quad [N] \quad (8)$$

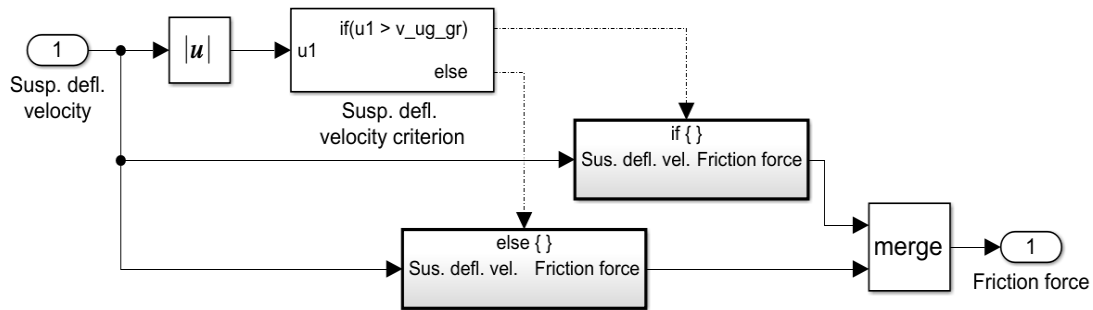


Fig. 9. Friction force calculation subsystem
Susp. defl., suspension deflection; vel., velocity

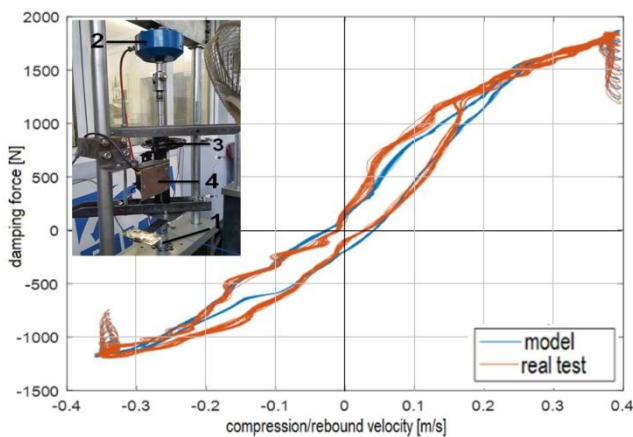


Fig. 10. Damper forces from the experimental test performed with the presented stand (1 – material test system [MTS] electrohydraulic excitator, 2 – force transducer, 3 – tested damper, 4 – travel sensor) and modelled

Forces modelled by the static non-linear model with added hysteresis and friction modules are presented in Fig. 10 and compared with the results from the experiment, as presented in the photograph in Fig. 10. Experimental tests of the characteristics of the three various types of shock absorbers, using a material test system (MTS) electrohydraulic actuator, performed by one of the authors, are described in a previous publication (11).

The comparison of damping forces calculated from static characteristics with those calculated from friction and hysteresis

modules shows that the influence of including friction and hysteresis should be much bigger for lower frequencies due to their much larger share in the total damping force, as seen in Figs. 11 and 12.

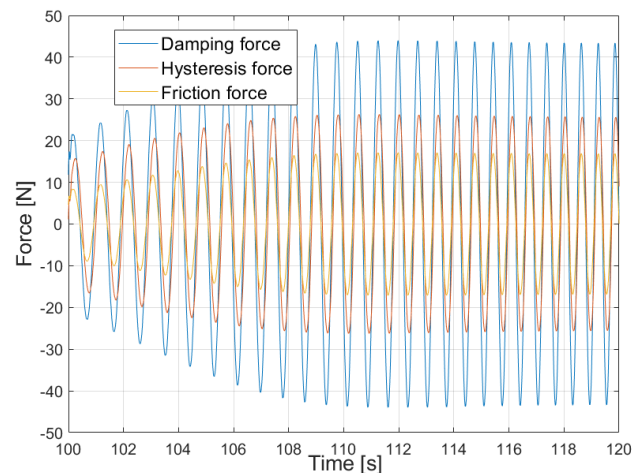


Fig. 11. Comparison of damping forces calculated from static characteristics with those calculated from friction and hysteresis modules for the first resonant frequency, which is approximately equal to 1 Hz

As previously stated, there were a few versions of a quarter-car model used in the research: one only static and linear version, which was set to maximum damping force; one with minimum

force (reference model); and six versions of advanced models – linear and non-linear, which had switched-on modules of friction, hysteresis, or friction and hysteresis.

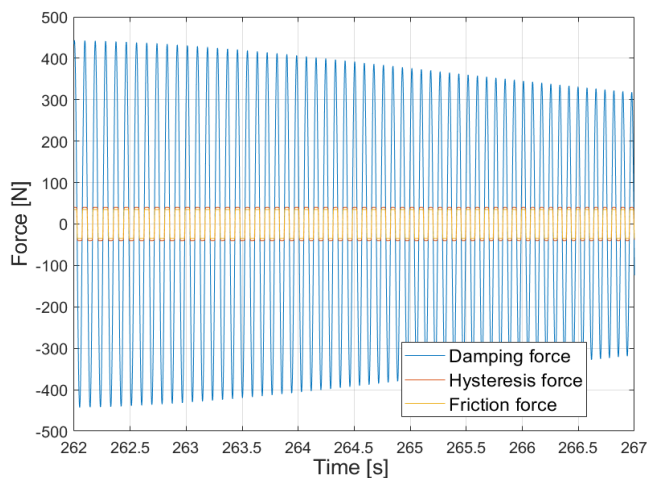


Fig. 12. Comparison of damping forces calculated from static characteristics with those calculated from friction and hysteresis modules for the second resonance: approximately 11 Hz

3. METHODOLOGY FOR ANALYSIS OF THE TESTING AND SIMULATION RESULTS

In the simulation tests, a quarter-car model that includes a non-linear damper model with controllable friction and hysteresis modules, which could be turned on or off, was used. Besides the damper module, the remainder of the model was linear, with the parameters of the model presented in Tab. 2. For each variant, the same excitation was applied – a changing-frequency sine wave of amplitude 3 mm, with the course of frequency’s variability shown in Fig. 3.

The influence of friction and hysteresis implemented separately or simultaneously was analysed for three indicators: 1) suspension deflections; 2) cumulative force between the tyre and the road surface; and 3) sprung mass accelerations for linear passive dampers and non-linear passive dampers. The analysed indicators allow for the evaluation of the suspension performance in terms of ride comfort, ride safety and rattle space of suspension required for its work. The tools chosen for the analysis of suspension performance were the transfer functions (frequency responses) between the given indicator and the kinematic excitation. They were chosen because these indicators are not defined by a single value but are expressed as a function of the excitation frequency.

These functions were calculated using the response signals (deflection, cumulative tyre force and sprung mass acceleration) obtained during simulations, as would be done for an experimental testing of suspension frequency responses. These functions between particular responses and kinematic excitation were calculated using the MatLab tfestimate function. The reason why these functions were not calculated analytically using suspension element parameters was the non-linear character of the damper model. The resulting frequency responses were then plotted as graphs, which show their magnitude as a function of frequency, with frequencies ranging from 0.5 Hz to 25 Hz being investigated. The results for the relative values between a given case and the reference model also were used.

4. RESULTS

4.1. Influence of friction and hysteresis on a linear damper with minimum damping coefficient

The investigation began by analysing the influence of inclusion of friction force, hysteresis and their combined effects on a suspension with the simplest possible damping characteristic – passive linear one with minimum (900 Ns/m) and maximum (3,100 Ns/m) damping coefficient. This was meant both to test the method of creating the transfer function graphs and to observe the effects of hysteresis and friction on the frequency response of a model. This resulted in the overall shape and behaviour of the linear damper matching the expectations and theory that was previously presented in literature (3,12) (blue characteristics in Figs. 13–18) – the reference transfer function for the model considering only the damping force.

First, the influence of friction force, hysteresis and their combined effects on the behaviour of the linear damper of minimum assumed damping, with damping coefficient of 900 Ns/m (dimensionless damping coefficient of 0.13) was analysed.

The resulting transfer functions for the suspension deflection are shown in Fig. 13.

For other suspension performance assessment criteria, analogous information was extracted from the graphs for the most crucial frequencies:

- sprung mass resonant frequency – approximately 1 Hz;
- unsprung mass resonant frequency – approximately 10 Hz;
- frequency between resonances for sprung and unsprung masses – approximately 3 Hz; and
- maximum tested frequency – 25 Hz.

The relative values were calculated as the ratio between a given dynamic response’s value for a damper model with friction, hysteresis or both of them over the corresponding value for a simplified model (only static damper characteristics).

The suspension deflection transfer function analysis showed that adding hysteresis and friction to the damping force yields similar results as the increasing of the damping coefficient – for minimal damping, lowering the magnitude from 3.2 m/m to around 1.9 m/m for the first resonant frequency and from 3 m/m to 2.5 m/m for the second frequency (Fig. 13a).

Comparing the suspension deflection transfer function values for the four chosen frequency ranges, it is visible that the biggest influence of friction and hysteresis can be seen for unsprung and (especially) sprung mass resonant frequencies, with hysteresis affecting the results more than does friction (Fig. 13b – in relation to the reference model).

The next analysis was done for the transfer function of cumulative tyre force, which is synonymous with the contact force between the road and the tyre, which is used as an indicator for ride safety criteria. Adding friction and hysteresis decreases the values of the transfer function in the first and second resonance ranges: in the first, even to almost 40%; in the second, from about 6% to 12% (Fig. 14). The biggest influence is for the frequencies between the first and second resonances – from 40% to 90% increase – but the absolute values are still much smaller (>10 times) than for the second resonance.

The analysis of transfer function of sprung mass acceleration (Fig. 15), which is used as an indicator for the ride comfort criterion, shows that the influence of friction and hysteresis is visible for

three of the four analysed frequency ranges. For two of them, the sprung mass acceleration is greater than for the reference model. For the sprung mass resonant frequency range, the trend is reversed – the accelerations are smaller in value, which translates

to a better ride comfort for low frequencies, while being worse for higher ones. Once again, hysteresis plays a bigger role than friction for all frequencies.

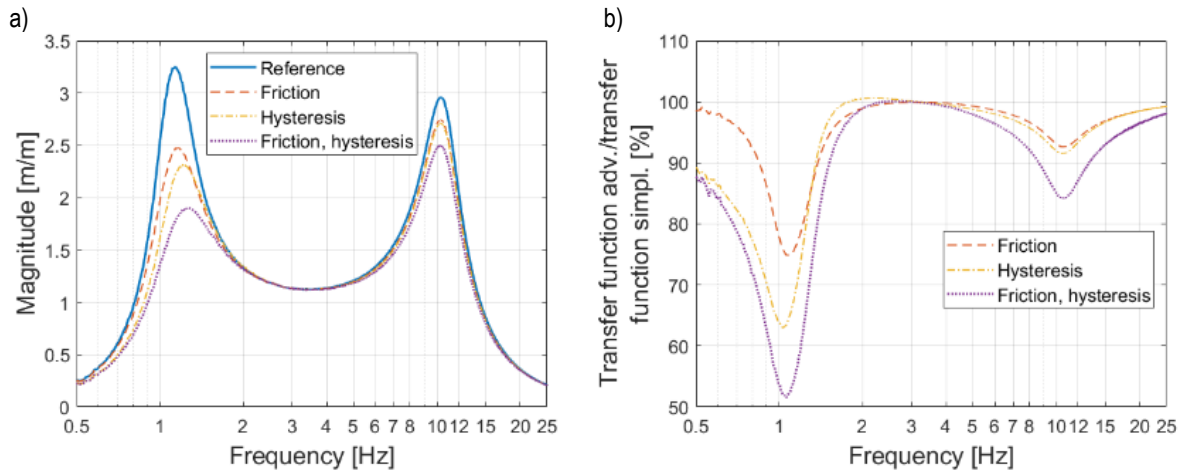


Fig. 13. Transfer function (a) between road excitation and suspension deflection and ratio (b) between suspension deflection transfer functions of reference (simpl.) and tested (adv.) models for minimal linear damping - 900 Ns/m (adv., advanced; simpl., simplified)

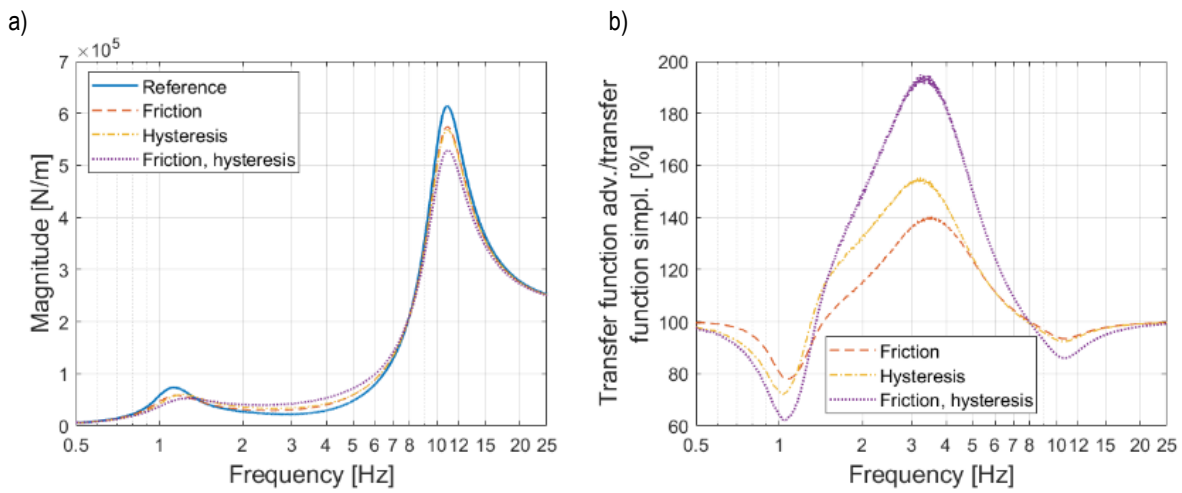


Fig. 14. Transfer function (a) between road excitation and cumulative tyre force and ratio (b) between cumulative tyre force transfer functions of reference (simpl.) and tested (adv.) models for minimal linear damping - 900 Ns/m (adv., advanced; simpl., simplified)

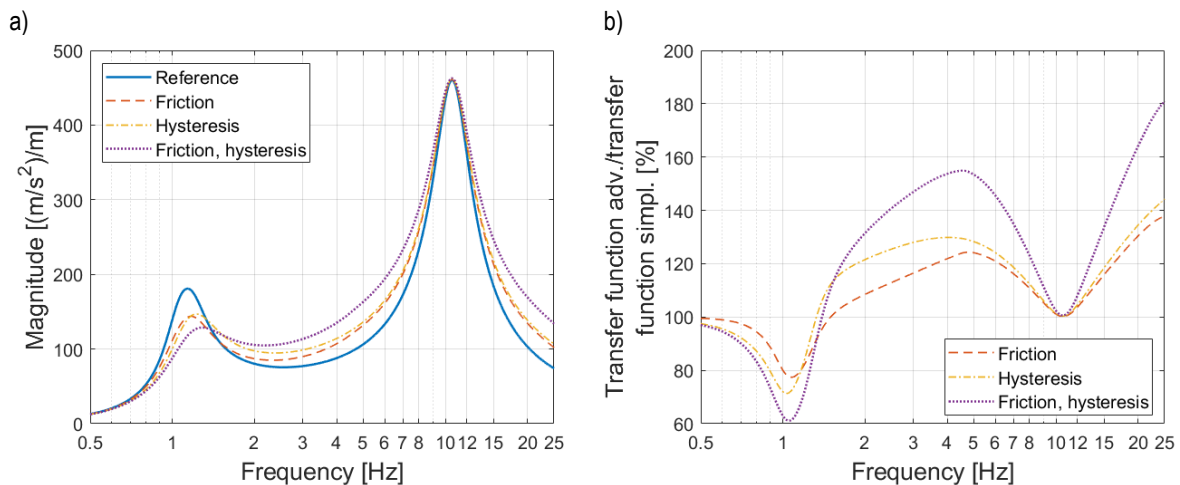


Fig. 15. Transfer function (a) between road excitation and sprung mass acceleration and ratio (b) between sprung mass acceleration transfer functions of reference (simpl.) and tested (adv.) models for minimal linear damping - 900 Ns/m (adv., advanced; simpl., simplified)

4.2. Influence of friction and hysteresis on a linear damper with maximum damping coefficient

Similarly to the linear damper of the minimum damping coefficient, the influence of the components of an advanced damper model on the transfer functions for different dynamic responses was analysed for a suspension with linear damping of maximum damping coefficient of 3,100 Ns/m (dimensionless damping coefficient of 0.45).

In the case of maximal damping and suspension deflection transfer function analysis (Fig. 16), it is visible that adding hysteresis (which also had a bigger effect on the minimal damping case than friction) causes the gain to drop to <math><1.1\text{ m/m}</math> for all frequencies and removes two separate resonances, leaving the one around 3 Hz.

The suspension deflection transfer function values for the four analysed frequency ranges and the comparison for those frequencies with the reference model (Fig. 17) show that the range

around 3 Hz is not sensitive to the inclusion of friction and hysteresis. For ranges of lower and higher frequencies, the influence of hysteresis is much bigger than the influence of friction. Hysteresis decreases the amplitudes of the first resonance about 40% and of the second about 25%, while reducing friction by about 10% and 7%, respectively (Fig. 17).

The next transfer function analysed was the cumulative tyre force for maximum linear damping. Compared to the minimum damping coefficient, a big difference is visible for low frequencies (Fig. 14 vs Fig. 17). In the first resonant frequency, the transfer function values are actually greater for the more advanced model by around 25% (Fig. 17), while for minimal damping, they are lower by around the same amount for friction and hysteresis, and even almost 40% lower for friction and hysteresis (Fig. 14). Friction's influence is also less pronounced for all frequencies, which is linked with its maximum value (35 N) being smaller, in comparison with the damping forces for higher damping coefficients.

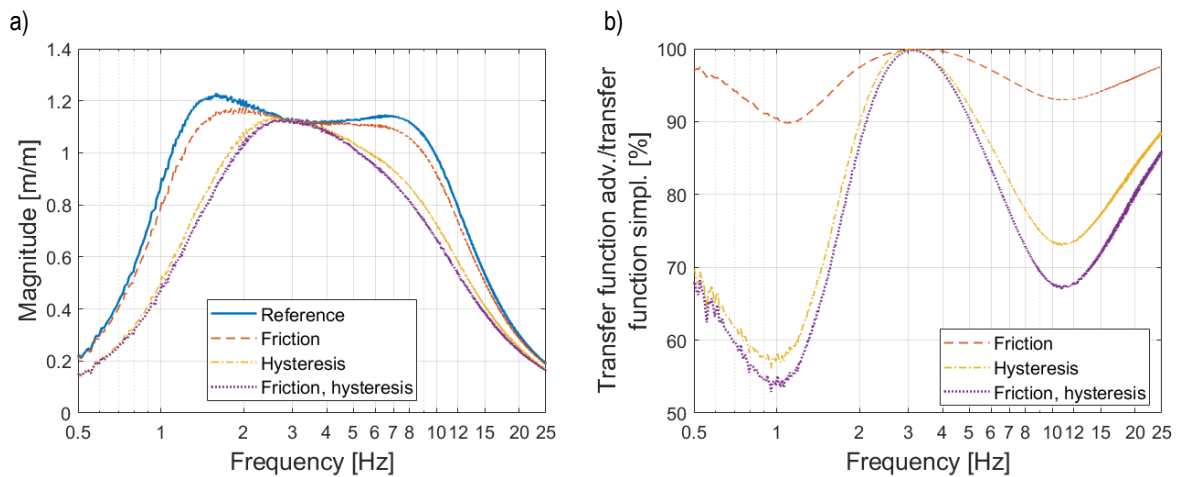


Fig. 16. Transfer function (a) between road excitation and suspension deflection and ratio (b) between suspension deflection transfer functions of reference (simpl.) and tested (adv.) models for maximal linear damping – 3,100 Ns/m (adv., advanced; simpl., simplified)

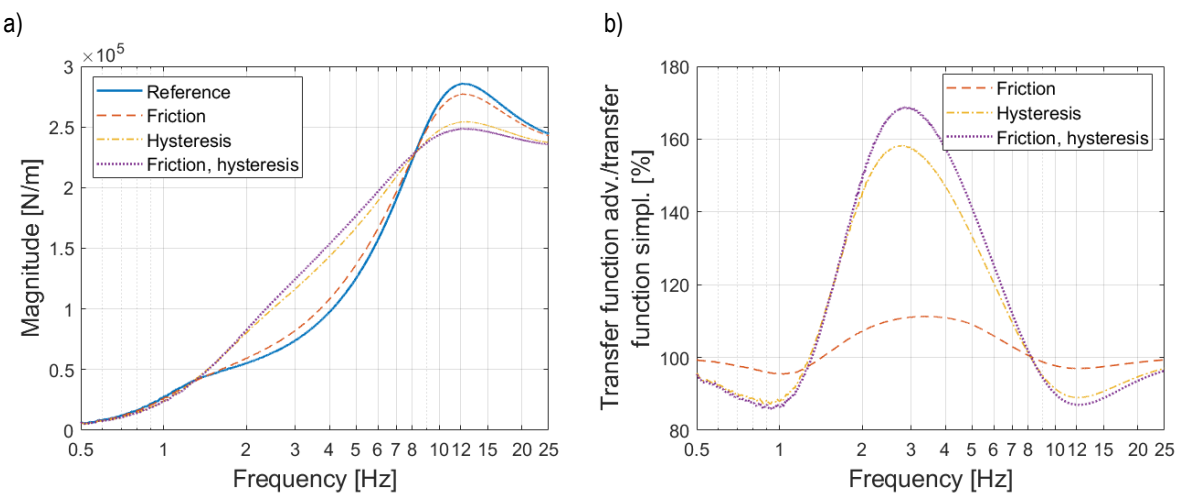


Fig. 17. Transfer function (a) between road excitation and cumulative tyre force and ratio (b) between cumulative tyre force transfer functions (adv., advanced; simpl., simplified)

The results for sprung mass accelerations are similar to those for the cumulative tyre force for 1 Hz, while the higher frequencies show higher influence of friction and hysteresis for almost all

cases compared to the results for minimum linear damping (Fig. 18). The effects are best visible for 3 Hz, while also being very noticeable for 25 Hz. For all frequencies, the transfer function

values are higher than in a reference model, indicating higher sprung mass accelerations, which translates to lower ride comfort.

Seeing these effects, a question arose regarding whether it is possible to find an equivalent damping coefficient, which could be used instead of more complicated models with friction and hysteresis modules. Simulation was conducted for a number of

values (Fig.19), and the results suggest that finding just one value that could simulate the behaviour of a model with friction and damping is impossible – big differences will arise either in the first or second resonant frequency. The potential solution to this problem would be the use of bilinear models, which have been previously extensively studied (8).

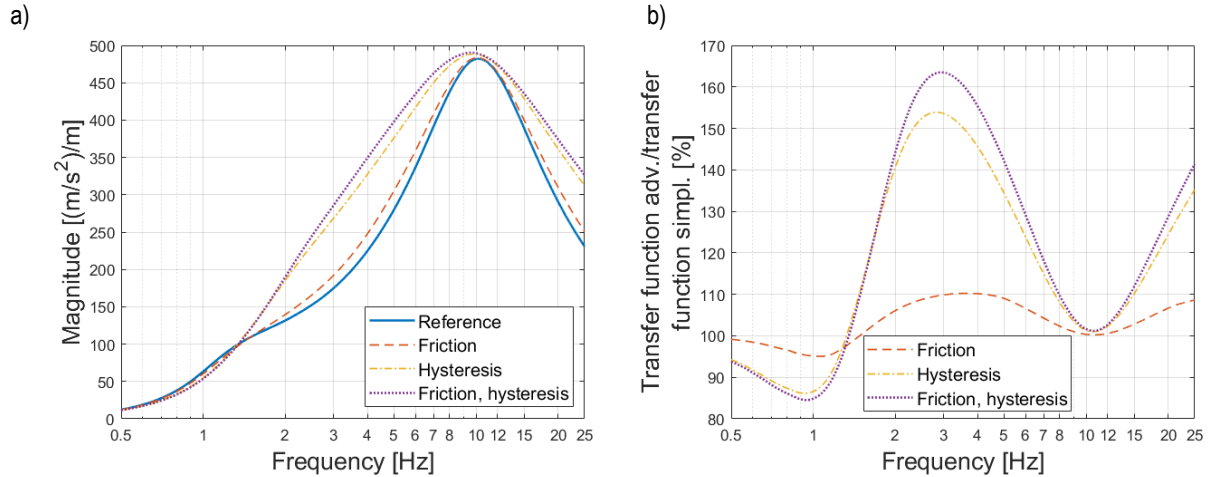


Fig. 18. Transfer function (a) between road excitation and sprung mass acceleration and ratio (b) between sprung mass acceleration transfer functions of reference (simpl.) and tested (adv.) models for maximal linear damping – 3,100 Ns/m (adv., advanced; simpl., simplified)

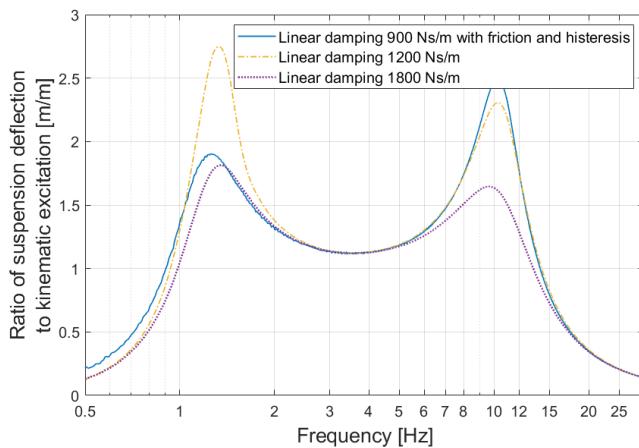


Fig. 19. Search for equivalent linear damping to friction and hysteresis - damping coefficient 1,800 Ns/m and 1,200 Ns/m

4.3. Influence of friction and hysteresis on a non-linear damper with the lowest damping mode

The next step was to look at the effects of friction and hysteresis on passive models that had non-linear characteristics implemented – for both the highest and the lowest possible damping modes. The results proved to be similar to those achieved in a fully linear model – friction and hysteresis acted as if the damping force was increased. It can be also observed that the total effect of both those forces is almost equal to a sum of both of them for all analysed suspension responses. Both friction and hysteresis had a slightly bigger impact near the first resonant frequency for minimal damping mode, decreasing the values of all analysed responses – tyre force, suspension deflection and both sprung

mass acceleration and displacement.

For the minimum non-linear damper model, the influence of friction and hysteresis on suspension deflections is less pronounced than for a linear model for 1 Hz, while being almost identical in other frequencies (Fig. 20). In general, the influence of a more advanced model does not exceed 20% for the minimum damping non-linear model.

Hysteresis and friction do not show a substantial influence on the cumulative tyre forces for the minimum damping non-linear model (especially compared to the linear version), the biggest effects being seen for the 3-Hz range, where the transfer function is higher by 35% for both forces implemented into the model.

For the remaining frequencies, the resulting cumulative tyre force transfer functions are slightly lower than in the reference model (Fig. 21).

Transfer functions for sprung mass accelerations show slightly bigger influence of friction and hysteresis (Fig. 22). The difference is that models with friction and hysteresis have transfer functions bigger than the reference model – especially for 3 Hz and 25 Hz.

Summarising the analysis for all responses, we can state that as the frequency rises, all the relations between the transfer functions shifted to values >1 (meaning that the dynamic responses for model with friction and/or hysteresis were greater than those for the reference ones), with the exception of suspension deflection, which remained <1 for the entire range. Maximum gain was achieved for all transfer functions for 3 Hz. After the first resonant frequency, the response for the maximum damping model was slightly greater compared to that for minimal damping – being smaller by 5–10 percentage points in the maximum for the model with both friction and hysteresis.

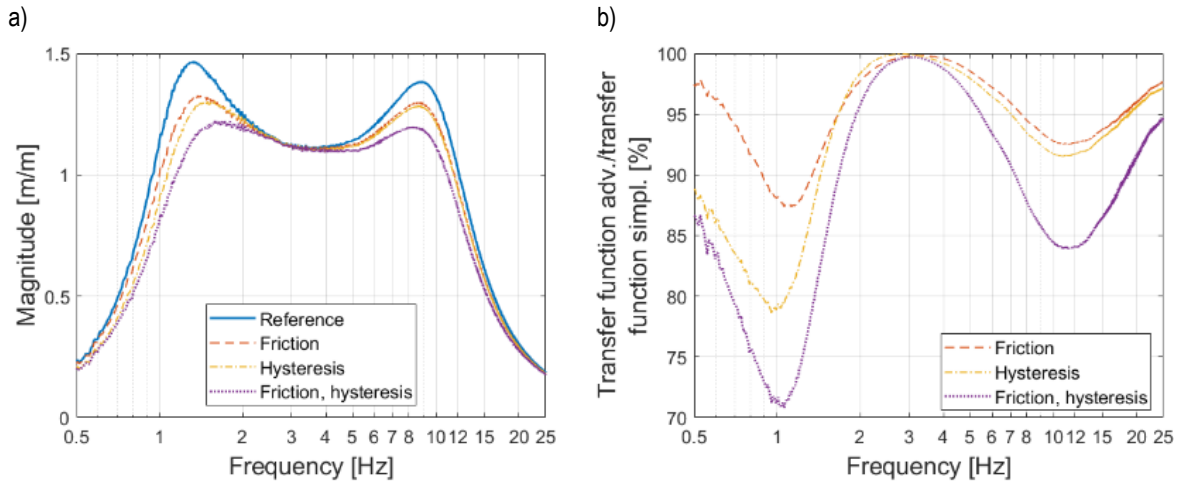


Fig. 20. Transfer function (a) between road excitation and suspension deflection and ratio (b) between suspension deflection transfer functions of reference (simpl.) and tested (adv.) models for minimal non-linear damping (adv., advanced; simpl., simplified)

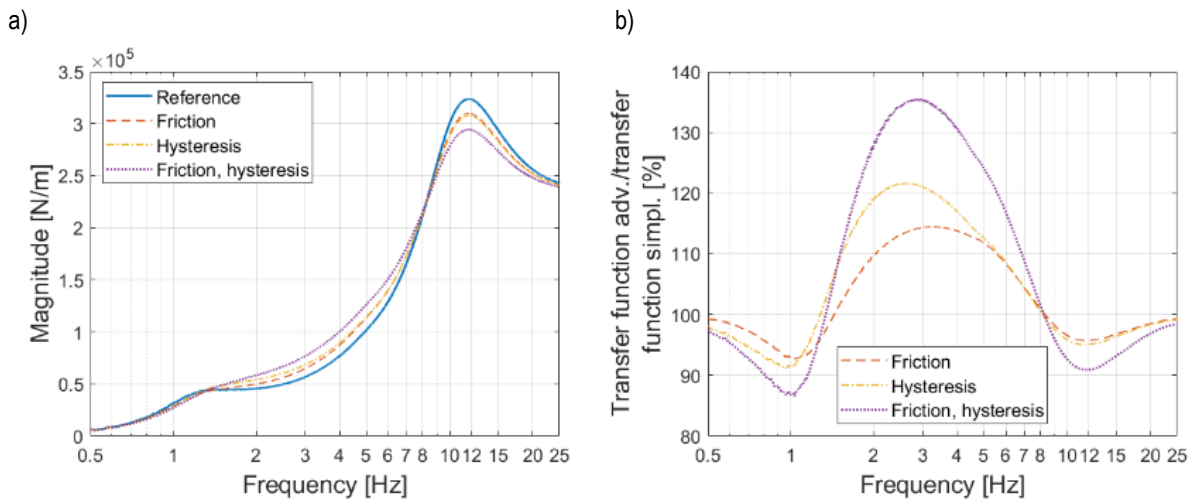


Fig. 21. Transfer function (a) between road excitation and cumulative tyre force and ratio (b) between cumulative tyre force transfer functions of reference (simpl.) and tested (adv.) models for minimal non-linear damping (adv., advanced; simpl., simplified)

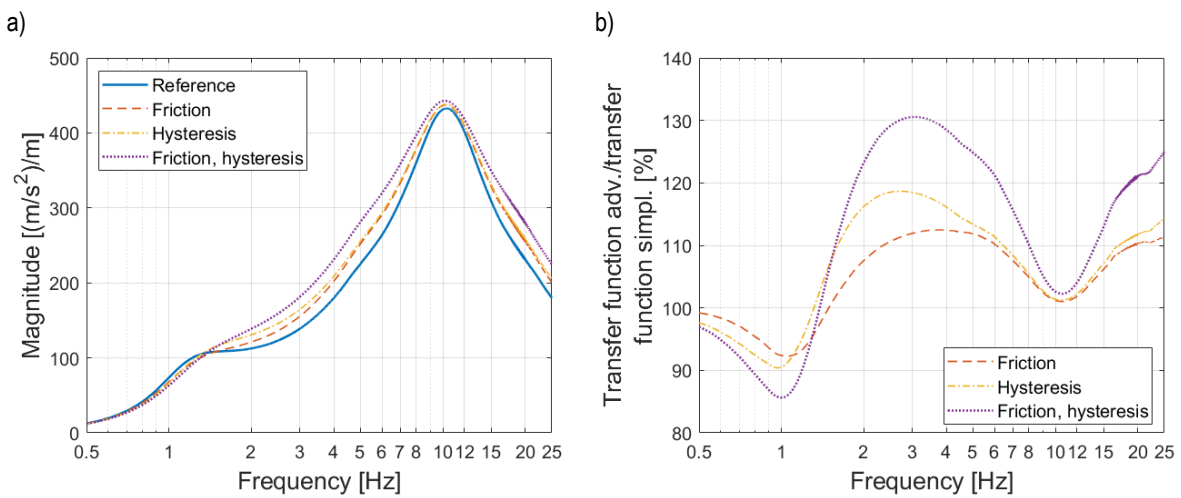


Fig. 22. Transfer function (a) between road excitation and sprung mass acceleration and ratio (b) between sprung mass acceleration transfer functions of reference (simpl.) and tested (adv.) models for minimal non-linear damping (adv., advanced; simpl., simplified)

4.4. Influence of friction and hysteresis on a non-linear damper with highest damping mode

For the maximum non-linear damping model, the effects of hysteresis are much more visible for the entire range of frequencies, with the exception of frequencies around 3 Hz (Fig. 23). This

influence ranges from 32% for the first resonance to around 22% for the second resonance, while the influence of friction does not exceed 6%. Additional elements in the damper model for suspension deflection cause the transfer function values to drop below reference values.

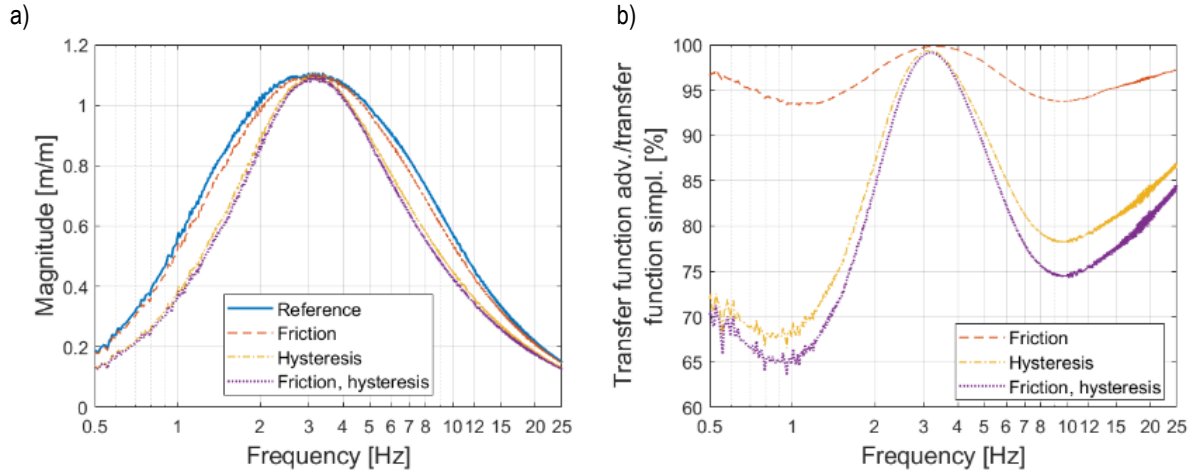


Fig. 23. Transfer function (a) between road excitation and suspension deflection and ratio (b) between suspension deflection transfer functions of reference (simpl.) and tested (adv.) models for maximal non-linear damping (adv., advanced; simpl., simplified)

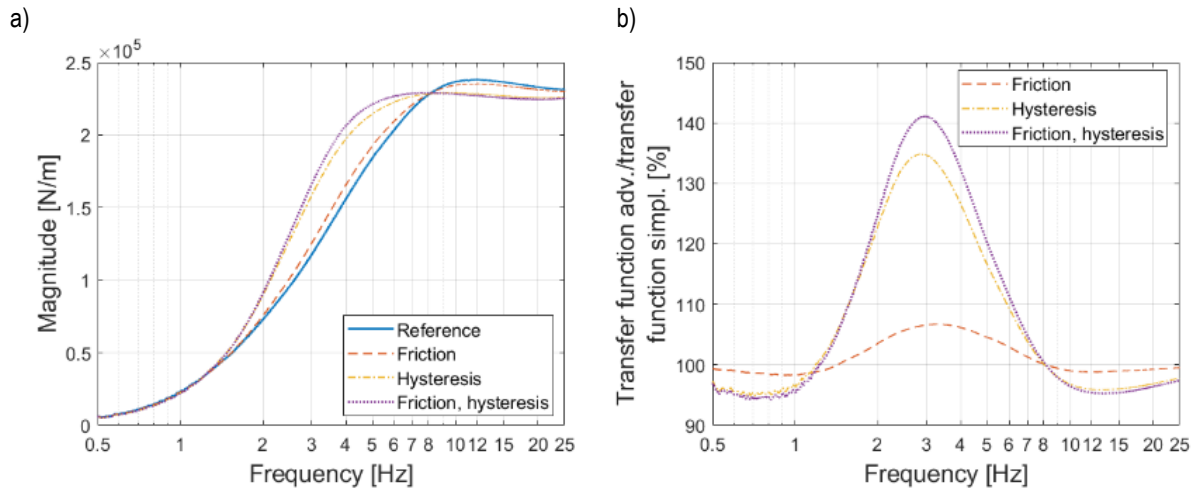


Fig. 24. Transfer function (a) between road excitation and cumulative tyre force and ratio (b) between cumulative tyre force transfer functions of reference (simpl.) and tested (adv.) models for maximal non-linear damping (adv., advanced; simpl., simplified)

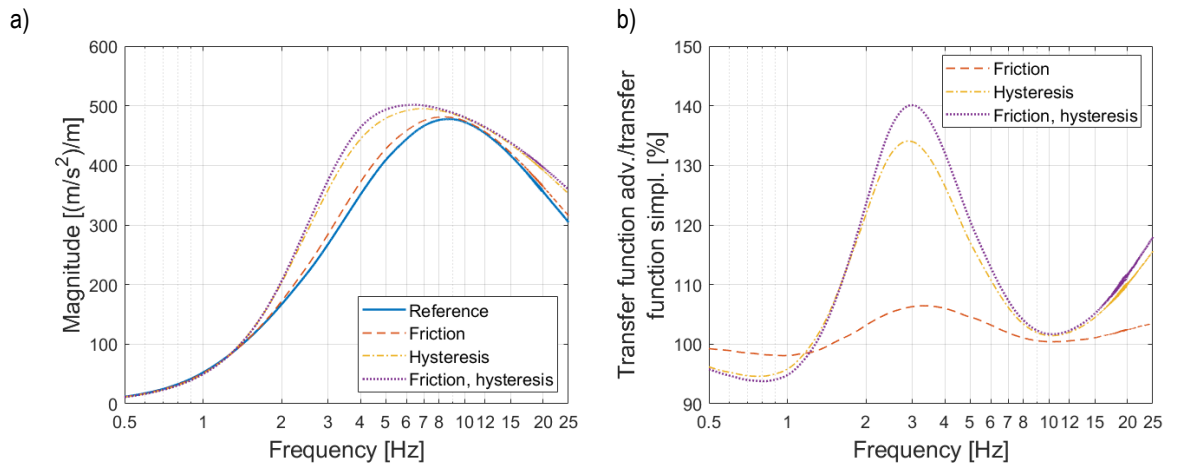


Fig. 25. Transfer function (a) between road excitation and sprung mass acceleration and ratio (b) between sprung mass acceleration transfer functions of reference (simpl.) and tested (adv.) models for maximal non-linear damping (adv., advanced; simpl., simplified)

The relative values for the maximum non-linear model's cumulative tyre force (Fig. 24) are analogous to the ones for minimum non-linear damping – the transfer function values are greater for the 3-Hz range while remaining almost unchanged for the remaining frequencies. Hysteresis once again has a bigger impact than friction.

The transfer functions for sprung mass accelerations show a slightly bigger influence of friction and hysteresis (Fig. 25). The difference relative to the cumulative tyre force is that the influence of friction and hysteresis is similar to and slightly bigger for the ranges of approximately 1 Hz and 3 Hz, bigger for approximately 10 Hz and much bigger for approximately 25 Hz.

5. SUMMARY RESULTS

After the analysis of each of the four cases (minimum linear, maximum linear, minimum non-linear and maximum non-linear), a synthesis of the influence was done. For better visualisation of the influence of friction, hysteresis and both combined on different indicators of suspension performance, summary charts were prepared (Figs. 26–28). These charts present the results of the relative values between a given case and the reference model for four chosen frequencies – near the first resonant frequency (ap-

proximately 1 Hz), 3 Hz, the second resonant frequency (around 10 Hz) and the maximum tested frequency (25 Hz).

Suspension deflection transfer functions are less sensitive to added friction or hysteresis in the range between the first and second resonances. The biggest influence is visible for the first resonance (approximately 1 Hz), whereby adding friction decreases the transfer function values from 25% to 48% compared to the linear static model. The influence for the non-linear minimum damping is smaller – the decrease is about 13%–29%.

The second resonance shows a smaller influence – the decrease is from 7% to 15% for linear models and from 6% to 26.33% for non-linear models. Changes in the values of the transfer functions for the frequencies about 25 Hz are similar to those for the second resonance, but the influence is half the value (3%–15%) for non-linear models and much smaller compared to linear models (1%–6%).

The transfer functions for the cumulative tyre forces are most sensitive to added friction or hysteresis in the range between the first and second resonances. Added friction or hysteresis increases the transfer function values from 7% to 92% compared to the linear static model. The biggest influence is observed for the minimal damping models – especially the minimum damping linear model.

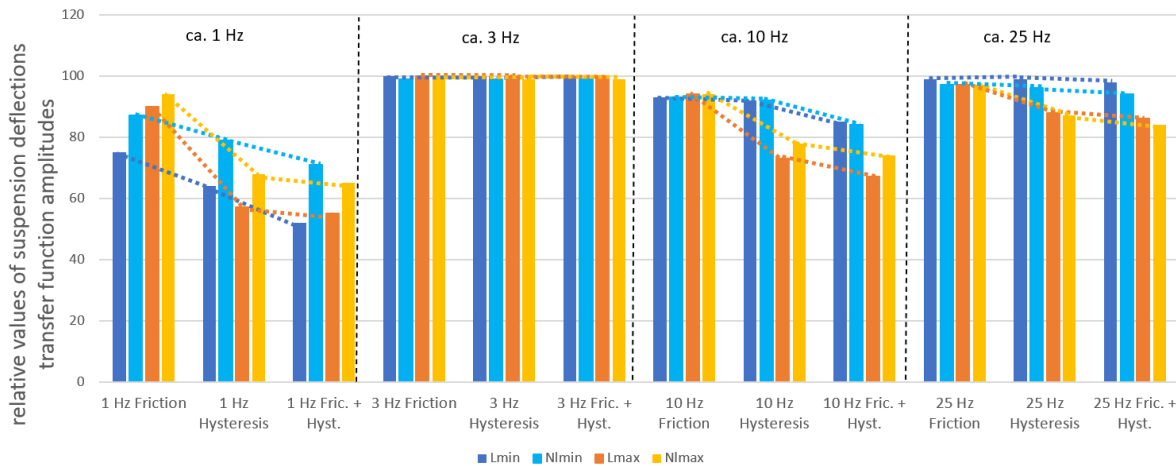


Fig. 26. Relations of the suspension deflection transfer function values of the tested (adv.) model to the values of the reference (simpl.) models for different damping characteristics and models at selected frequency regions (adv., advanced; simpl., simplified)

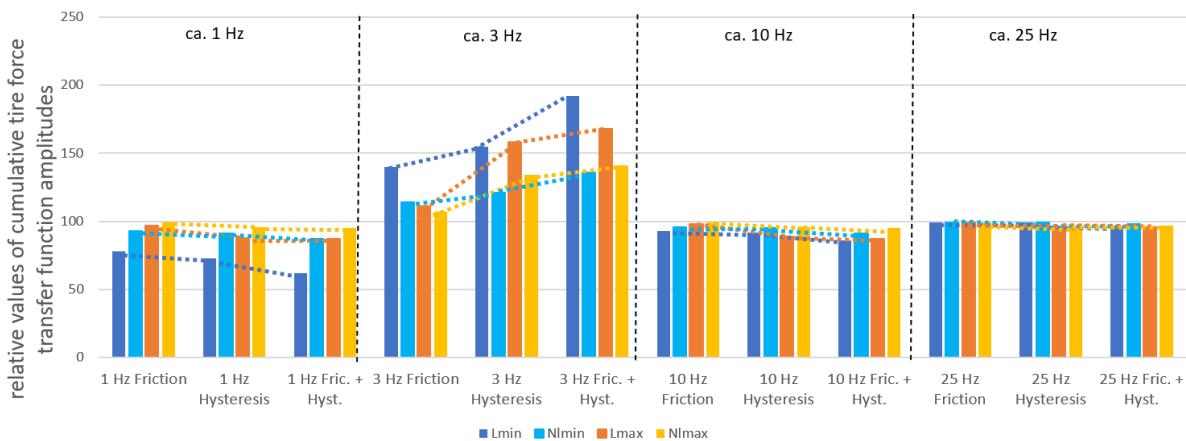


Fig. 27. Relations of the cumulative tyre force transfer values of the tested (adv.) model to the values of the reference (simpl.) models for different damping characteristics and models at selected frequency regions (adv., advanced; simpl., simplified)

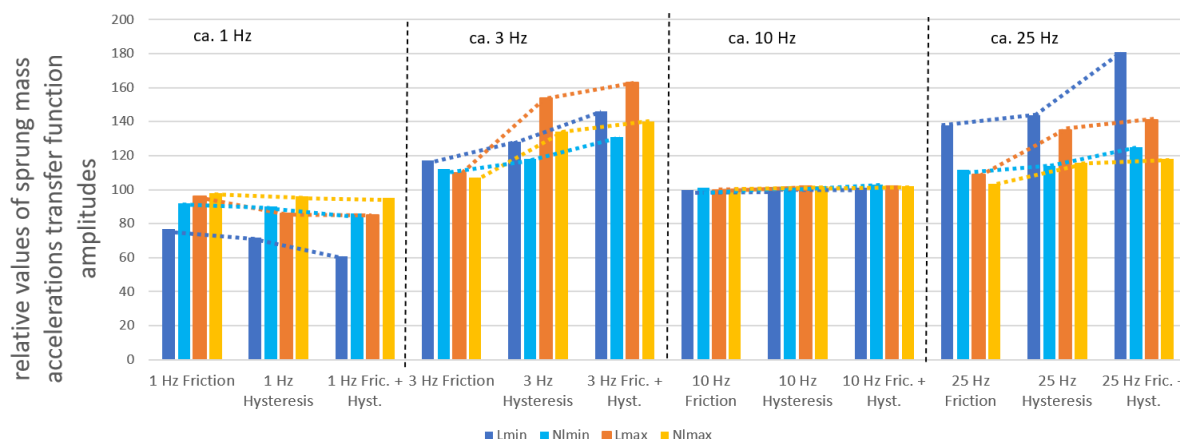


Fig. 28. Relations of the sprung mass acceleration transfer function values of the tested (adv.) model to the values of the reference (simpl.) models for different damping characteristics and models at selected frequency regions (adv., advanced; simpl., simplified)

The next level of influence is in the first resonance – it results in a decrease of the transfer function values from 22% to 38% for the minimum linear model and from 1% to 23% for the other models. It is less visible for the maximum damping non-linear model.

In the range of the second resonance (unsprung mass resonance), adding friction and hysteresis also decreases the transfer function values but by a lesser extent – from 4% to 14% for the minimal damping linear models and from 1% to 9% for the maximal damping linear models.

In the case of sprung mass accelerations used to assess the ride comfort, the increase in transfer function values are visible in the range between the first and second resonances and around the 25 Hz range. This increase is bigger for the minimum damping models – from 12% to 63% for the first resonance range and from 9% to 81% for the range of approximately 25 Hz.

There is almost no influence on the sprung mass transfer function values in the range of the second resonance – only a small increase of about 1%–3% is seen. For the range of the first resonance, a small decrease is visible.

6. CONCLUSION

During the research, the influence of inclusion of friction, hysteresis and combined friction and hysteresis into models of linear and non-linear damping forces on the three most important dynamic responses of a passive quarter-car suspension was tested.

The obtained results allow the assessment of this influence in both qualitative and quantitative ways. The quantitative influence is described in more detail in the “Results” and “Summary results” sections.

In general, it can be assumed that the effect of including friction and hysteresis gives an effect similar to that found on increasing the damping force; however, this effect is not linear, which results from the different influence of additional forces in the cases of low and higher operating speeds of the shock absorber (Figs. 11 and 12).

The differences in the influence of added friction and hysteresis are, in general, similar for both the minimum and maximal damping characteristics of the tested models. Bigger changes are visible between the minimum linear and non-linear models due to the fact that the linear model has a low damping coefficient for all working speeds. In the case of the non-linear model, for the low-

est speed, the damping coefficient is higher than for the higher speed (Fig. 4).

In the case of suspension deflection transfer functions, the addition of friction and hysteresis for all frequencies decreases or does not change (in the range of approximately 3 Hz) the transfer function values. The biggest decrease (up to almost 48% compared to the reference linear model) is observed for the first resonance, then for the second resonance and then the range of approximately 25 Hz.

In the case of the cumulative tyre force, which is used to assess the safety potential, the biggest negative impact on safety is visible in the range of approximately 3 Hz. However, in that range, only the relative gain is large. The absolute values of this transfer function for the said frequency range are small in general, and the only important one is the second resonance range (approximately 10.12 Hz) – the decrease in the amplitudes of the transfer function is from 2% to 14% for linear and from 1% to 9% for non-linear damping characteristics.

For assessing comfort, the sprung mass acceleration transfer function is used, and the range of the second resonance is the most important as the absolute values of this function are the biggest. Added friction and hysteresis cause only a small (1%–3%: Fig. 28) increase. A much bigger influence (increase by 63% to 81%) is found for ranges of approximately 3 Hz and approximately 25 Hz. Yet, the absolute values are much smaller than for the second resonant frequency.

The research shows the importance of including the proposed modules (friction and hysteresis) in the damper model analysing the transfer functions for passive dampers. It can explain some differences observed between the dynamic responses of suspension models with only static characteristics and responses of a real suspension. This is all the more important because, currently, hydraulic gas-pressure shock absorbers with non-linear static characteristics are used in modern cars.

REFERENCES

1. Ślaski G. Studium projektowania zawiesznień samochodowych o zmiennym tłumieniu. Wydawnictwo Politechniki Poznańskiej. Poznań: Wydawnictwo Politechniki Poznańskiej; 2012. 399–404 p.
2. Grajert J. Izolacja drgań w maszynach i pojazdach. Wydawnictwo Politechniki Wrocławskiej; 1997.

3. Mitschke M. Dynamika samochodu t.2 Drgania. Warszawa: Wydawnictwo Komunikacji i Łączności; 1989.
4. Reński A. Bezpieczeństwo czynne samochodu. Zawieszenia oraz układy hamulcowe i kierownicze. Oficyna Wydawnicza Politechniki Warszawskiej; 2011.
5. Zdanowicz P, Lozia Z. Wyznaczenie optymalnej wartości współczynnika asymetrii amortyzatora pasywnego zawieszenia samochodu z wykorzystaniem modelu „ćwiartki samochodu”. Pr Nauk Politech Warsz Transp. 2017;(119):249–65.
6. Zdanowicz P. Ocena stanu amortyzatorów pojazdu z uwzględnieniem tarcia suchego w zawieszeniu. Politechnika Warszawska; 2012.
7. Lyu D, Zhang Q, Lyu K, Liu J, Li Y. Influence of the Dry Friction Suspension System Characteristics on the Stick-Slip of Vertical Vibration of a Three-Piece Bogie. Shock Vib. 2021;2021.
8. Ślaski G, Klockiewicz Z. the Influence of Shock Absorber Characteristics' Nonlinearities on Suspension Frequency Response Function Estimation and Possibilities of Simplified Characteristics Modelling. Arch Automot Eng. 2022;96(2):77–95.
9. Dąbrowski K. Algorytmizacja adaptacyjnego sterowania tłumieniem zawieszenia samochodu dla uwzględnienia zmienności warunków eksploatacji. 2018.
10. Kwok NM, Ha QP, Nguyen TH, Li J, Samali B. A novel hysteretic model for magnetorheological fluid dampers and parameter identification using particle swarm optimization. Sensors Actuators, A Phys. 2006;132(2):441–51.
11. Więckowski D, Dąbrowski K, Ślaski G. Adjustable shock absorber characteristics testing and modelling. IOP Conf Ser Mater Sci Eng. 2018;421(2).
12. Savaresi SM, Poussot-Vassal C, Spelta C, Sename O, Dugard L. Semi-Active Suspension Control Design for Vehicles. 2010.

 Zbyszko Klockiewicz:  <https://orcid.org/0000-0003-4353-550X>

 Grzegorz Ślaski:  <https://orcid.org/0000-0002-6011-6625>